N O T I C E

THIS DOCUMENT HAS BEEN REPRODUCED FROM MICROFICHE. ALTHOUGH IT IS RECOGNIZED THAT CERTAIN PORTIONS ARE ILLEGIBLE, IT IS BEING RELEASED IN THE INTEREST OF MAKING AVAILABLE AS MUCH INFORMATION AS POSSIBLE

NASA

Technical Memorandum 81982

Initial Assessment of the Effects of Energetic Ion Injections in the Magnetosphere Due to the Transport of Satellite Power System Components from Low Earth Orbit to Geosynchronous Earth Orbit

S. A. Curtis and J. M. Grebowsky

JULY 1980

National Aeronautics and
Space Administration

Goddard Space Flight Center
Greenbelt, Maryland 20771

DEC 1980
RECEIVED
NASA STI FACILITY
ACCESS DEPT.

(NASA-TM-81982) INITIAL ASSESSMENT OF THE EFFECTS OF ENERGETIC ION INJECTIONS IN THE MAGNETOSPHERE DUE TO THE TRANSPORT OF SATELLITE POWER SYSTEM COMPONENTS FROM LOW EARTH ORBIT TO GEOSYNCHRONOUS EARTH ORBIT

N81-12682

Unclas
G3/46 39827

Initial Assessment of the Effects of Energetic Ion Injections in the Magnetosphere Due to the Transport of Satellite Power System Components from Low Earth Orbit to Geosynchronous Earth Orbit

S.A. Curtis and J.M. Grebowsky
Laboratory for Planetary Atmospheres

NASA/Goddard Space Flight Center
Greenbelt, Maryland 20771

July 1980

This work is supported by the Dept. of Energy/Argonne National Laboratory
Interagency Agreement No. DE-AI02-80CH10048

Abstract

Potentially serious environmental effects exist when cargo orbital transfer vehicle (COTV) ion propulsion is used on the scale proposed in the preliminary definition studies of the Satellite Power System. These effects of the large scale injections of ion propulsion exhaust in the plasmasphere and in the outer magnetosphere are shown to be highly model dependent with major differences existing in the predicted effects of two models--the ion cloud model and the ion sheath model. The expected total number density deposition of the propellant Ar^+ in the plasmasphere, the energy spectra of the deposited Ar^+ and time-dependent behavior of the Ar^+ injected into the plasmasphere by a fleet of COTV vehicles differ drastically between the two models. The major environmental effect of the former model is communication disturbance due to plasma density irregularities (Curtis and Grebowsky, 1980b), in contrast to the spectacular predictions of the latter model which include power line tripping and pipe line corrosion (Chiu et al., 1979b). The ion sheath model is demonstrated to be applicable to the proposed Ar^+ beam physics if the beam is divergent and turbulent whereas the ion cloud model is not a realistic approximation for such a beam because the "frozen-field" assumption on which it is based is not valid. Finally, it is shown that the environmental effects of ion propulsion may be mitigated by the appropriate adjustment of the beam parameters.

Introduction

In this initial assessment we have concentrated on understanding the physics of energetic ion beam propagation in the terrestrial magnetosphere. Such an understanding is essential in order that the potential environmental effects of the projected massive amounts of ion beam injections during Satellite Power System (SPS) construction may be evaluated. Although experimental ion beam injections in space are required for a full understanding of the beam physics, we believe that a realistic beam propagation model consistent with the underlying physics is needed. Toward this end we will compare and contrast two proposed models for the physics of the ion exhaust ejected by the cargo orbital transfer vehicle (COTV), namely: our ion beam sheath loss model (Curtis and Grebowsky, 1980a) and an ion cloud model used originally to describe barium release experiments in the magnetosphere (Scholer, 1970).

The possible environmental effects from the two proposed beam propagation models are radically different. For the ion beam sheath model we would expect a depletion of the high energy ions in the radiation belt (Curtis and Grebowsky, 1980b) whereas for the ion cloud model the trapped relativistic electrons would increase (Chiu et al., 1979b). The expected radiation belt dosages thus go in opposite directions depending on the model chosen. In addition, the extension of the radiation belts out to the geosynchronous orbit with the associated radiation dosage hazard for the Satellite Power System (Cladis and Davidson, 1980) is only possible in the ion cloud model with the much more massive deposition of thermal exhaust ions it predicts. Also, the generation of artificial ionospheric currents is a direct product of only the ion cloud model. If the assumption of frozen-in field lines does not hold

(which is to be expected in a manifestly turbulent plasma environment such as the exhaust ion beam), the validity of the ion cloud model and its spectacular enviromental effects such as power-line tripping and pipeline corrosion (Chiu et al., 1979b) would vanish. The major environmental effect that is expected from the ion beam sheath loss model that we have developed is the degradation of satellite communications; ground to space, space to ground and space to space. These communication disruptions are caused by small spatial irregularities produced by: (1) plasma instabilities in the plasmasphere driven by the energetic anisotropic ions shed by the beam during its propagation through the plasmasphere; and (2) by the precipitation of magnetospheric ions into the ionosphere by the shed beam ions.

Due to the drastic differences in the environmental impacts predicted by the two beam models, it is imperative that it be determined which of the models is consistent with the physics of the proposed COTV ion beam configuration. We will show that only the ion sheath loss model can adequately explain the physics of the beam. Later, we also discuss possible experiments to resolve beam physics and strategies that can be used to reduce environmental effects which may result from the beam injections.

Model Comparisons and their Related Environmental Effects

In lifting massive space power system payloads from low earth orbit to geosynchronous earth orbit, Cargo Orbital Transfer Vehicles (COTV) using ion propulsion will inject energetic beams of argon ions into the plasmasphere (Department of Energy, 1978). The characteristic speeds of the plasmasphere relevant for ion beam propagation are the Alfven speed and the ion thermal speed. Near the earth's equatorial plane, the argon ion beams have a speed $V_b \lesssim V_A$, the plasmasphere Alfven speed, and $V_b >> V_{th}$, the plasmasphere ion's thermal speed (see Figure 1). The Alfven speeds are shown for the Chiu et al. (1979a) model plasmasphere and the average and low Alfven speeds are calculated from OGO-5 observations analyzed by Chen et al. (1976). As can be seen, the Chiu et al. model gives an upper bound to the Alfven speeds. The average OGO-5 Alfven speeds give the best current indication of the Alfven speeds which are of the order of the beam speed throughout most of the equatorial plasmasphere whose outer boundary is between 4 and 6 earth radii (R_e). Hence $V_b \lesssim V_A$. The thermal speeds in Figure 1 are taken from the Chiu et al. model. In this case discrepancies between observations and the model are unimportant since $V_b >> V_{th}$ always.

Another characteristic velocity needing consideration in beam modelling is the spread of the beam velocity perpendicular to its direction of propagation. In the case of the SPS COTV, the spread of the beam velocity perpendicular to its direction of propagation is $\Delta V_b \approx 0.4V_b$ (Hanley and Guttman, 1978) as shown in Figure 2--this corresponds to approximately 20° in angular spread and only a 3% loss of effective thrust due to the divergence of the beam. This spread is comparable to

those currently attainable, e.g. a half angle of $\sim 15^{\circ}$ corresponding to only a 2% thrust loss due to divergence is characteristic of the 30 cm Hg systems already developed (D.C. Byers, personal communication). Thus, the exhaust of the COTV's may be described as a fast, rapidly diverging ion beam. Despite these facts, theories have been developed recently (Y. T. Chiu and H. B. Liemohn, private communication) which assume that the emerging COTV exhaust will have a very small velocity spread. However, the arguments underlying the assumptions of these theories are based on laboratory experiments whose applicability to the problem of ion beam exhaust injection into the plasmasphere remains to be demonstrated. In particular, the finite geometries in the laboratory experiments induce wall effects which will affect beam spread. In addition if the beam is not completely neutralized but contains a substantial net current, classical z-pinch (Boyd and Sanderson, 1969) effects will occur which will tend to compress the beam. Finally, the laboratory experiments were apparently done in parameter regimes with magnetic fields, and Alfvén speed to beam speed ratios that are not characteristic of the plasmasphere. Given these facts, the beam must be regarded as rapidly diverging until relevant experiments in space can demonstrate otherwise. Due to these beam characteristics, the numerous potential plasma instabilities which could take energy from the beam and hence stop it are ineffective. This is due to the fact that the beam and background plasma parameters change sufficiently rapidly so as not to allow amplification of instability generated waves to significant amplitudes. The interested reader is referred to Curtis and Grebowsky (1980a) where a quantitative discussion is given of the criteria needed for instabilities to be a significant beam stopping mechanism.

Another proposed beam stopping theory (Chiu et al., 1979b) models the fast ion beam as a slowly moving ion cloud with $V_b << V_{th}$ and $V_b << V_A$. This is not applicable given the relationship of V_b to V_A and V_{th} shown in Figure 1. In addition, this ion cloud model assumed the beam plasma can be regarded as infinitely conducting. This frozen field line concept however is not valid since a realistic model of the beam plasma (Ichimaru, 1973) which accounts for both the initial plasma turbulence and that generated by the low amplitude plasma wave turbulence carried with the beam gives rapid diffusion times $\tau = \lambda_D^2/D^*$ as shown in Figure 3. Note that λ_D is the beam ion Debye length and D^*, the anomalous diffusion coefficient associated with the plasma turbulence,

$$D^* \approx \frac{1}{32\pi} \frac{c}{e\beta} (T_e T_i)^{1/2} (1 + T_i/T_e)^{3/2} \ln (m_i/m_e) \qquad (1)$$

where T_i and T_e are the ion and electron beam temperatures in energy units and m_i and m_e, the corresponding masses. The currents resulting from the turbulence-induced anomalous resistivity are insufficient to short out the polarization electric field given the range of values of ΔV_b. This is true since for a quasi-perpendicularly propagating ion beam the current driven by the polarization electric field, $E_p \approx \frac{V_b}{c} B$ is given by

$$J = \sigma^* E_p \qquad (2)$$

where $\sigma^* \sim \omega_b^2/4\pi\langle\upsilon\rangle$, $\langle\upsilon\rangle = \lambda_D^{-2} D^*$, where $\omega_b = \left(\frac{4\pi n_b e^2}{m_e}\right)^{1/2}$ is the beam electron plasma frequency and $\lambda_D = \left(\frac{T_i}{4\pi n_b e^2}\right)^{1/2}$ is the beam ion Debye length. Then since $J = n_b e V_c$ the current velocity is given by:

$$V_c = \frac{\sigma^* V_b B}{n_b e c} \qquad (3)$$

and since we require $\Delta V_b > V_c$ for the polarization electric field not to be shorted out we obtain the condition

$$\frac{\sigma^* B}{n_b ec} \frac{V_b}{\Delta V_b} < 1 \tag{4}$$

for beam propagation. For the expected values of $\Delta V_b/V_b$ (Hanley and Guttman, 1978) we do not expect the polarization field to be shorted out and hence the beam will propagate. Equation (4) also explains why barium releases are often not observed to propagate very far: the initial ejection is nearly radial from the explosion point making the spread of the velocity normal to the radial direction small and hence allowing a rapid shorting out of the polarization field. In addition, given the slower rate of density decrease in the barium releases, plasma instabilities will be effective in stopping such releases. We emphasize that the beam stopping is always a strong function of the initial conditions and thus very different behavior may be exhibited by different release experiments. Thus, the stopping processes assumed in the ion cloud models are not needed to stop either beams or releases.

Since significant plasma turbulence and an effectively infinite plasma conductivity cannot exist simultaneously, ion beam propagation models which include both the ion cloud mechanism and plasma instabilities (Chiu et al., 1979b) are not self consistent. Also ion cloud models based on the analysis of Scholer (1970) require that the beam's perpendicular velocity spread be zero or very near it, since the model treats the beam plasma as an incompressible fluid. Since ion thruster exhausts are known to possess large velocity spreads (Hanley and Guttman, 1978), this is yet another reason why ion cloud models are not applicable

to the case of ion beam propagation in the plasmasphere or in any plasma system except those in which the parameters change at unrealistically slow rates.

Despite the limitations imposed on beam stopping mechanisms by the beam velocity characteristics and its finite conductivity, not all of the COTV beam plasma will escape the plasmasphere. Since the polarization electric field imposed at the thruster to allow cross-field propagation of the beam is nonuniform over the sheath of the beam (see figure 4), the plasma in this sheath is lost and deposited on local field lines. This model is discussed in detail in Curtis and Grabowsky (1980a). The beam sheath formation is a natural consequence of the termination of the polarization field at the sheath's outer edge. A beam sheath loss model describing this process predicts a deposition of argon ions and hence energy in the plasmasphere which is much less than that in models which call for ion cloud mechanisms or plasma instabilities to rapidly stop the beam. In Figure 5, a comparison is given of the cumulative fractional mass loss of an ion beam injected at 1.5 R_e for the ion cloud model and the ion beam sheath loss model. The ion cloud process stops the beam very rapidly whereas all but a few percent of the beam in the ion beam sheath loss process escapes. In Figure 6 the integrated difference of these two deposition models is shown for the construction of one SPS. The ion cloud process results in more than an order of magnitude greater energy and number density deposition than that of the sheath loss process. The energy spectra of Ar^+ deposited in the plasmasphere are also dissimilar. For the ion cloud model accompanied by a weaker plasma instability loss process the solid line in Figure 7 gives a qualitative indication of the

energy spectra (Chiu et al., 1979b) of the argon ions. In the ion cloud model, most of the energy of Ar^+ is dissipated in producing ionospheric currents caused by the cloud's field line dragging. This process yields the low energy peak. The higher energy tail and peak just below the injection energy of ∿5 keV would be produced by various instability processes. In contrast, the sheath loss model shown by the dotted line in Figure 7 results in deposited Ar^+ with energies near the injection energy.

The ion cloud and ion beam sheath loss models also produce very different Ar^+ plasmasphere densities as a function of time. In the ion cloud model the exhaust of a COTV stops rapidly and the time dependent Ar^+ injection is local. In contrast, the ion beam sheath loss model gives time dependent Ar^+ injection that is not localized but rather is extended a number of earth radii away. Thus, when the COTV fleet starts transportation from LEO to GEO of SPS construction materials, the Ar^+ COTV exhaust is rapidly deposited throughout the plasmasphere in the ion beam sheath loss model. However, in the ion cloud model the Ar^+ deposition will be localized and move as a front with the COTV fleet.

To quantify this discussion, we consider the specific case of the Department of Energy (1978) scenario for COTV transport of SPS materials using silicon photo-voltaic cells. In this scenario, it is projected that there will be 15 COTV flights per SPS over approximately a 135 day time period. Assuming the launches to be equally spaced in time from LEO (i.e., at time intervals of 9 days) we have done a computer simulation of the time dependent Ar^+ plasmasphere density distribution as a function of time from the first COTV launch from LEO. The assumed dominant loss channel for the Ar^+ is charge exchange with the neutral background exosphere. This appears to be the dominant loss channel from our previous work (Curtis and Grebowsky, 1980a) and is taken in the computer simulation as the e-folding time for the decay of the injected Ar^+. In the calculations the relatively small Ar^+ injection stemming from the COTV fleet return

to LEO from GEO is neglected. This is equivalent to assuming that the COTV fleet is disassembled at GEO for use in SPS construction rather than being reused. The calculation is applicable only to distances within approximately four earth radii of LEO because outside of the plasmasphere loss processes other than charge exchange may dominate--such as plasma convective loss during substorms.

In Figure 8 is shown the radial position of a COTV as a function of time from LEO departure. As can be seen from the figure, the injections are greater nearer earth (L less than 2.5) than in the more distant plasmasphere. This effect is greatly reduced however by the much lower Ar^+ charge exchange lifetimes in the inner region (Curtis and Grebowsky, 1980a). The solid circles indicate the radial position of the members of a fleet of COTV's when the first COTV reaches GEO assuming a LEO launch approximately every 9 days.

Using the trajectory depicted in Figure 8 the computer simulation yields the results in Figure 9. The Ar^+ density distributions are shown at selected time intervals of 27, 72 and 133 days for both the ion cloud and ion beam sheath loss models. Although the near-LEO Ar^+ deposition is greater for the ion cloud model than the beam sheath loss model, the sheath model gives a much larger spatial extent for the Ar^+ deposition. Due to the much shorter charge exchange lifetimes near LEO the total remnant plasmasphere Ar^+ deposition at day 27 by the ion cloud model does not exceed the ion sheath loss deposition by as much as the total deposition difference between the models. Later, at day 72, the ion cloud model still is spatially localized near LEO, whereas the sheath loss model is characterized by significant deposition throughout the plasmasphere. At day 133, all the materials for the construction of one SPS are delivered to GEO and a continuing fleet of COTV's to supply the materials for the second SPS are enroute. At this time the Ar^+ densities predicted for the ion cloud model are much greater than those for the sheath model. The distinct dip in the radial distribution near L = 2.5 is due to the lengthening of lifetimes with respect to charge exchange in the outer plasmasphere and to the increase in

L-shell volume in the outer plasmasphere. These effects combine to produce the plateau in the Ar^+ density in the outer plasmasphere. The Ar^+ density plateau at $2.5 \lesssim L \lesssim 5.0$ (nominal plasmapause position) will be the long term signature of the Ar^+ plasmaspheric deposition. The inner plasmasphere charge exchange lifetimes are sufficiently short so as to give a rapid relaxation of Ar^+ back to its natural plasmasphere density which is negligible. We note that away from LEO the solid angle subtended by the earth decreases from 2π steradians (a full hemisphere). Thus at greater distances more of the hot neutral Ar atoms created by the charge exchange process will escape into space rather than be recycled into the terrestrial atmosphere.

In Figure 10 is shown a continuation of the computer simulation in time beyond that shown in Figure 9. The construction materials for a second SPS are now being ferried to GEO. We show the resulting time dependent Ar^+ plasmasphere densities as a function of radial distance for times of 160, 205, and 266 days after the first COTV left LEO with the first SPS construction materials. In continuing the simulation to the second SPS, it is assumed that the second SPS is the last to have materials transported up to day 266. The plots in Figure 10 then depict the relaxation of the Ar^+ densities as the inner source terms are removed to successively greater distances--that is, the last member of the COTV fleet with construction materials moves outward through the plasmasphere. The Ar^+ densities are again plotted for both the ion cloud and the ion beam sheath loss models. For both models, the inner plasmasphere densities drop precipitously after the COTV exhaust source is removed. However, the outer plasmasphere Ar^+ density plateau persists due to the long Ar^+ lifetimes with respect to charge exchange in that region. Throughout the plasmasphere during these times, the ion cloud model yields much greater Ar^+ densities than the sheath loss model. This has direct implications for environmental effects which scale with the magnitude of the Ar^+ density.

In summary, from these computer simulations of the Ar^+ density resulting from COTV exhaust injection into the plasmasphere we have the following conclusions:

1) During the construction of the first SPS, the ion beam sheath loss gives an Ar^+ density enhancement of much greater spatial extent than the ion cloud model which produces a perturbation which moves like a wave with the COTV through the plasmasphere. The reason for this is that in the ion cloud model the beam is stopped in a short distance compared to the plasmasphere scale size, whereas in the sheath loss model the beam is not stopped.

2) At later times, after the first COTV reaches GEO, a substantial Ar^+ density plateau develops in the outer plasmasphere. It is much greater for the ion cloud model than for the ion beam sheath loss model.

3) The outer plasmasphere Ar^+ density plateau will tend to persist for long time periods given the long charge exchange lifetimes. For a similar reason, the inner plasmasphere Ar^+ is rapidly depleted.

In terms of environmental effects, when the results of the computer simulation are combined with the differences of the energy spectra of the two models, the ion beam sheath loss model may be expected to produce greater possible communication perturbations during the initial transport of materials to GEO for the first SPS. This results from the fact that greater numbers of energetic ($\sim$ 5 kev) Ar^+ ions will exist over larger spatial extents than in the ion cloud model since the beam is not stopped locally.

Later studies of the Ar^+ time dependent plasmasphere densities should include the consideration of longer term processes involving loss by pitch angle scattering and plasmasphere dynamics. This will allow a better

assessment of the magnitude of the outer plasmasphere Ar^+ density plateau in a multiple SPS construction scenario.

In our ion beam sheath loss model we have assumed that the Debye length is given by an effective temperature which is proportional to the square of the beam spread velocity (Curtis and Grebowsky, 1980a). In essence this implies a rapid thermalization of the perpendicular velocity spread of the beam. Since the ion beam emerging as the COTV exhaust is expected to be turbulent upon emission due to the beam creation and charge neutralization processes, the turbulence implies a rapid randomization of the perpendicular velocity spread component. In particular, in the charge neutralization process electrons will be injected with the ions in the thruster. The differences in velocity in directions perpendicular to the ion beam propagation in the electron and ion distribution functions may then be expected to drive two-stream type plasma instabilities which will generate turbulence and randomize ΔV_b. It should be noted that the wave amplification process occurs on fixed shells (concentric to the beam axis) comoving with the ion beam and hence does not suffer from the limitation of wave amplification processes that seek to stop the beam itself (Curtis and Grebowsky, 1980a).

If the thermalization of ΔV_b by plasma instabilities is only partially successful, then the effective temperature will be less. Since our ion beam sheath loss model Ar^+ densities scale with the Debye length, they vary as the square root of the effective temperature. Partial thermalization could result in a factor of ten or more reduction in the Ar^+ density that the model predicts. This would make the predicted environmental effects of the ion beam sheath loss model even less severe when compared to the massive Ar^+ deposition envisioned in the ion cloud model. To better estimate the degree of beam velocity spread thermalization, a better specification of beam parameters such as emitted ion and electron velocity distribution functions is needed than are currently available.

The different beam stopping mechanisms can produce very different environmental impacts. The sheath loss model predicts a large injection of energetic anisotropic argon ions which will drive plasma instabilities which may produce sufficient scintillation to impair radio communications with geosynchronous satellites. The partial depletion by precipitation of the energetic ion belts surrounding the earth is also possible due to the pitch angle scattering caused by Ar^+ turbulence. A detailed description of potential environmental effects using the sheath loss model is given in Curtis and Grebowsky (1980b). Cold argon ions ($T \sim 1$ eV) are produced in the sheath loss model only via the loss of energy by plasma instability mechanisms and electron coulomb scattering. Since during the energy degradation processes, Ar^+ will be lost by charge exchange and precipitation, the amount of cold Ar^+ plasma from the sheath loss mechanism will be much less than from the ion cloud mechanism. The environmental effects due to cold Ar^+ would be greatly reduced in the sheath loss picture as well as those effects due to ionospheric currents (Chiu et al., 1979b). Specifically, with the greatly reduced numbers of cold Ar^+ expected in the ion sheath model, the dosage enhancement of trapped relativistic electrons predicted by Chiu et al. (1979b) would not occur. The extension of the radiation belt environment out to the geosynchronous region envisioned by Cladis and Davidson (1980) using the Chiu et al. (1979b) model would also not occur since it requires large cold ion deposition. The artificial ionospheric current predicted by the Chiu et al. model relies exclusively on the ion cloud model's frozen-in field lines being dragged. Without the very doubtful "frozen-in picture", the Chiu et al predicted powerline tripping and pipeline corrosion will not occur. To claim that results of the ion cloud and beam sheath loss

models are the same because the final state in both cases is to leave cold Ar^+ in the plasmasphere is meaningless. The radically different energy deposition spectra shown in figure 7 yield very different plasmasphere modifications before reaching their final state (cold Ar^+) by various energy degradation processes.

Relevant Experiments

To establish a convincing final assessment of the beam propagation physics, experimental tests are required to overcome the credibility problems. As Roger Bacon said in his work Opus Tertium, "The strongest of arguments prove nothing so long as the conclusions are not verified by experience." This is true in plasma physics in particular where experiment characteristically leads theory. From this viewpoint, a very good experimental test would be a Space Shuttle-born ion beam experiment. Remote in situ measurements of the ion beam characteristics could be done by a free flying satellite launched prior to the experiment by the space shuttle. This could be a scaled down COTV Ar^+ thruster with power levels of about a kilowatt and a nozzle diameter of a few centimeters rather than the COTV values of a megawatt and a meter respectively. The development of suitable advances in ion thrusters for such an experiment does not seem to pose major technical problems but is rather limited by the willingness to expend the necessary funding (Hudson and Finke, 1980). The other beam parameters could be the same as for a COTV. The down sized COTV thrusters would then have the same exhaust beam speed, perpendicular velocity spread, density and ion mass as the projected full sized COTV thrusters. The required power levels could be within the limits of the planned 20kW orbiter integral solar array or the 6kW orbiter mounted array (Franklin, 1980).

We emphasize that experimental conditions which do not closely correspond to those of the COTV ion beam exhaust will not give a meaning-

ful assessment of the exhaust physics. In particular, in order to be applicable, the ion mass, the initial beam density, the beam velocity and its perpendicular velocity spread as well as, the background plasma density, composition and magnetic field used in experiments must be near those expected in the case of COTV ion beam injection. Only in space can these conditions be well satisfied.

Mitigation Strategies

If the perpendicular velocity spread of the ion beam exhaust can actually be reduced, despite current engineering problems, to where $\frac{\Delta V_b}{V_b} \ll 1$, then plasma instabilities will become important in stopping the beam as discussed in Curtis and Grebowsky, (1980a). However this effect can be reduced by increasing $\Delta V_{b/V_b}$ and thus increasing $\dot{n}_{b/n_b}$ and not allowing large amplification of instabilities. Increasing $\Delta V_{b/V_b}$ may also be necessary to stop the turbulence driven currents from shorting out E_p and thus stopping the beam. This will, however, reduce the overall efficiency of the propulsion system since ΔV_b does not contribute in lifting cargo to higher orbits. When argon was chosen as the propellant the choice was based on its availability and the combination of high specific impulse and high thrust that using an intermediate mass ion allowed. Use of either a lighter or heavier mass ion would sacrifice these overall efficiencies. For a given beam energy, the beam velocity scales as $m_i^{-\frac{1}{2}}$ for a specific ion mass. Instability processes involving the beam are characteristically proportional to the beam ion plasma frequency $\omega_{pi} = (4\pi\, n_e^2/m_i)^{\frac{1}{2}}$ and the ion gyro-frequency $\Omega_i = eB/m_i c$. Thus $\Omega_i \propto m_i^{-1}$ and $\omega_{pi} \propto m_i^{-\frac{1}{2}}$. Plasma instabilities for a fixed beam energy can thus be suppressed by choosing a heavier mass ion since the allowed length for instability amplification is proportional to $V_b \omega_i^{-1}$ where the growth rate $\omega_i \propto \omega_{pi}$ or $\omega_i \propto \Omega_i$. Choice of a heavier ion will

however decrease the beam speed V_b for a fixed beam energy E_b, so it may also be necessary to increase E_b in order to suppress instabilities after the rapid beam expansion phase. In the later phase of beam propagation the restriction on instability growth lengths are given by the length scales of the convective derivatives discussed in Curtis and Grebowsky (1980a) that are related to inhomogenieties in the plasmasphere and are proportional to V_b. Increasing E_b may be necessary even without going to a heavier ion if plasma instabilities are effective in stopping the beam in the post-rapid expansion phase of its propagation.

Conclusions

Understanding the correct physics of propagation of the ion beam emitted by the COTV's envisioned for SPS is critical to assessing what environmental effects may occur. In the two models discussed here the underlying physics is very different as are the predicted environmental effects. We believe that our theory, which models the ion beam's propagation by a sheath loss model, is much more in accord with the present understanding of plasma physics than is the ion cloud model which assumes concepts such as "frozen-in" field lines without consideration of the restricted range in which the assumptions are valid. Our theory is also self consistent - in contrast, for the reasons mentioned above, the ion cloud model is not and (as applied to the COTV ion beam problem) often calls for the simultaneous operation of mutually exclusive processes. The major environmental effect that we foresee from our modelling of the COTV ion beams is communication impairment due to scintillations caused by ionospheric and plasmaspheric density irregularities. These irregularities are produced by the hot anisotropic argon ions deposited by the beam. The more spectacular effects predicted by the ion cloud model

will not occur or will be reduced in magnitude by many orders of magnitude due to the reduced deposition of beam ions deduced in the beam sheath model. Should technological advances require modifications to the system design of the COTV thrusters, the beam model developed by us can be used to determine how best to minimize the environmental impact through judicious selection of the free beam parameters.

We strongly feel that that appropriate space, as opposed to laboratory, experiments are needed. Since the capability to perform these studies will not be obtained until about the mid-80's, we recommend that additional theoretical work be done in order to lay a firm foundation for the questions to be addressed by the experiments. Specific theoretical work suggested includes both a more refined modelling of the ion beam propagation in the plasmasphere, of the deposition of beam ions in the plasmasphere, and of the time dependent overall plasmasphere response to this input.

REFERENCES

Boyd, T. M. J., and J. J. Sanderson, Plasma Dynamics, Barnes and Noble, Inc., New York, 1969

Chen, A. J., J. M. Grebowsky and K. Marubashi, Diurnal Variations of Thermal Plasma in the Plasmasphere, Planet. Space Sci., 24, 765, 1976.

Chiu, Y. T., J. G. Luhmann, B. K. Ching and D. J. Boucher, Jr., An Equilibrium model of Plasmaspheric Composition and Density, J. Geophys. Res., 84, 909, 1979a.

Chiu, Y. T., J. G. Luhmann, M. Schultz and J. M. Cornwall, Effects of Construction and Operation of a Satellite Power System Upon the Magnetosphere, Aerospace Report No. ATR-80 (7824)-1, 1 December 1979b.

Cladis, J. and G. T. Davidson, Magnetospheric Effects of Solar Power Satellite, Proceedings of Global Technology 2000 Meeting, Baltimore, MD, American Institute of Aeronautic and Astronautics, May, 1980.

Curtis, S. A. and J. M. Grebowsky, Energetic Ion Beam Magnetosphere Injection and the Solar Power Satellite J. Geophys. Res., 85, 1729, 1980a.

Curtis, S. A. and J. M. Grebowsky, Changes in the Terrestrial Atmosphere-Ionosphere-Magnetosphere System due to Ion Propulsion for Solar Power Satellite Placement, Space Solar Power Review, in press, 1980b.

Department of Energy, Satellite Power System (SPS) Concept Development and Evaluation Program, DOE ER-0023, October 1978.

Franklin, I.V., Solar Array Opportunities in the 1980's and Beyond, Journal of the British Interplanetary Soceity, 32, 42, 1980.

Hanley, G. and Guttman, C. H., Satellite Power Systems Concepts Definition Study: Final Report Executive Summary, Rockwell-International, Vol. I, 1978.

Ichimaru, S., Basic Principles of Plasma Physics: A Statistical Approach, W. A. Benjamin, Inc. (Advanced Book Program) Reading, Mass., 1973.

Scholer, M., On the motion of artificial ion clouds in the magnetosphere, Planet. Space Sci., 18, 1977, 1970.

FIGURE CAPTIONS

Figure 1. Comparison of the characteristic Alfven speeds and thermal ion speeds with the projected COTV argon ion exhaust speed as a function of distance in earth radii in the equatorial plane.

Figure 2. Diagram of expanding argon ion beam emitted by a COTV. The width of the beam sheath, the Debye length λ_D, is shown in an enlargement.

Figure 3. Diffusion time of magnetic field through the turbulent ion beam plasma. The field lines will rapidly slip through the beam rather than being "frozen-in".

Figure 4. Gradient of beam speed across the beam sheath due to the drop off of the polarization electric field over the Debye length λ_D. This gives a continual shedding of the beam sheath and hence yields the deposition of energetic, anisotropic argon ions in the plasmasphere.

Figure 5. Comparison of fraction of total mass of an ion beam deposited in the plasmasphere as a function of radial distance when the COTV is at 1.5 earth radii. Two beam models are shown: ion cloud and ion beam sheath loss.

Figure 6. Comparison of total number density of Ar^+ deposited in the plasmasphere for each SPS built. The ion cloud and ion beam sheath loss models are compared.

Figure 7. Comparison of the energy spectra of the Ar^+ deposited in the plasmasphere by the ion cloud and ion beam sheath loss models.

Figure 8. Radial position of a COTV carrying SPS construction materials as a function of time. The points on the curve indicate the radial positions of the members of a COTV fleet if launching occurs equally spread in time.

Figure 9. Time dependent deposition of Ar^+ in the plasmasphere for a COTV fleet carrying SPS construction materials from LEO to GEO. The silicon scenario SPS parameters are used here (Department of Energy, 1978) and the COTV's are assumed to depart from LEO in an equally spaced time sequence. Deposition for ion cloud and ion beam sheath models--the solid and dashed curves respectively--are compared.

Figure 10 Continuation of Figure 9 for the COTV transport of construction materials for a second SPS. The launchings from LEO are again assumed to be equally spaced in time and start with the first time interval after the last COTV for the first SPS is launched.

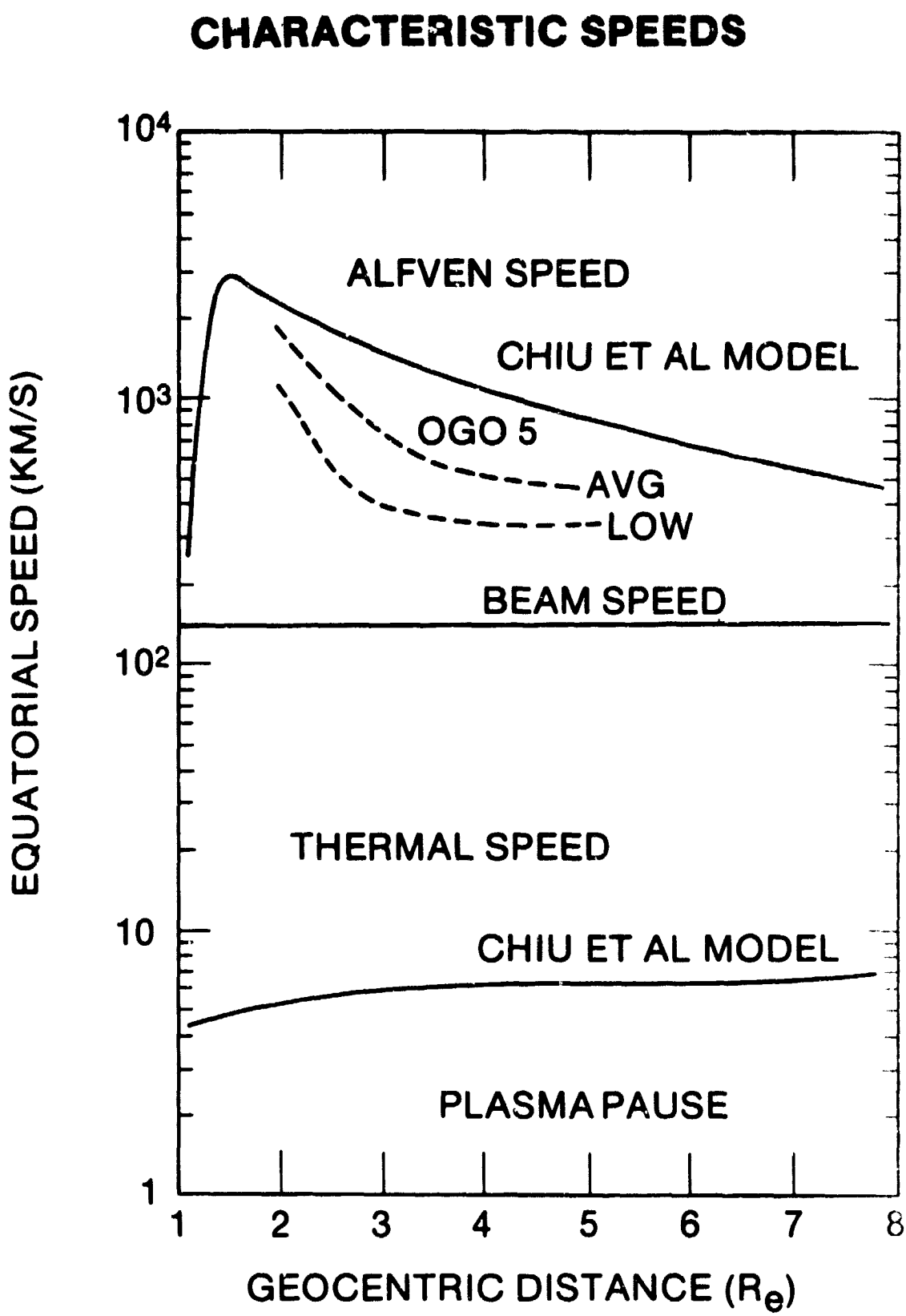
CHARACTERISTIC SPEEDS
ALFVEN SPEED
CHIU ET AL MODEL
OGO 5
AVG
LOW
BEAM SPEED
THERMAL SPEED
CHIU ET AL MODEL
PLASMA PAUSE
EQUATORIAL SPEED (KM/S)
GEOCENTRIC DISTANCE (R_e)
10^4
10^3
10^2
10
1
1
2
3
4
5
6
7
8

FIGURE 1

ION BEAM CROSS-SECTION

r_O = THRUSTER RADIUS

$V_B \approx 150$ Km SEC^{-1}

$\Delta V_B \approx 0.4\ V_B$

$\frac{\Delta V}{r_O} \approx 6 \times 10^4\ SEC^{-1}$

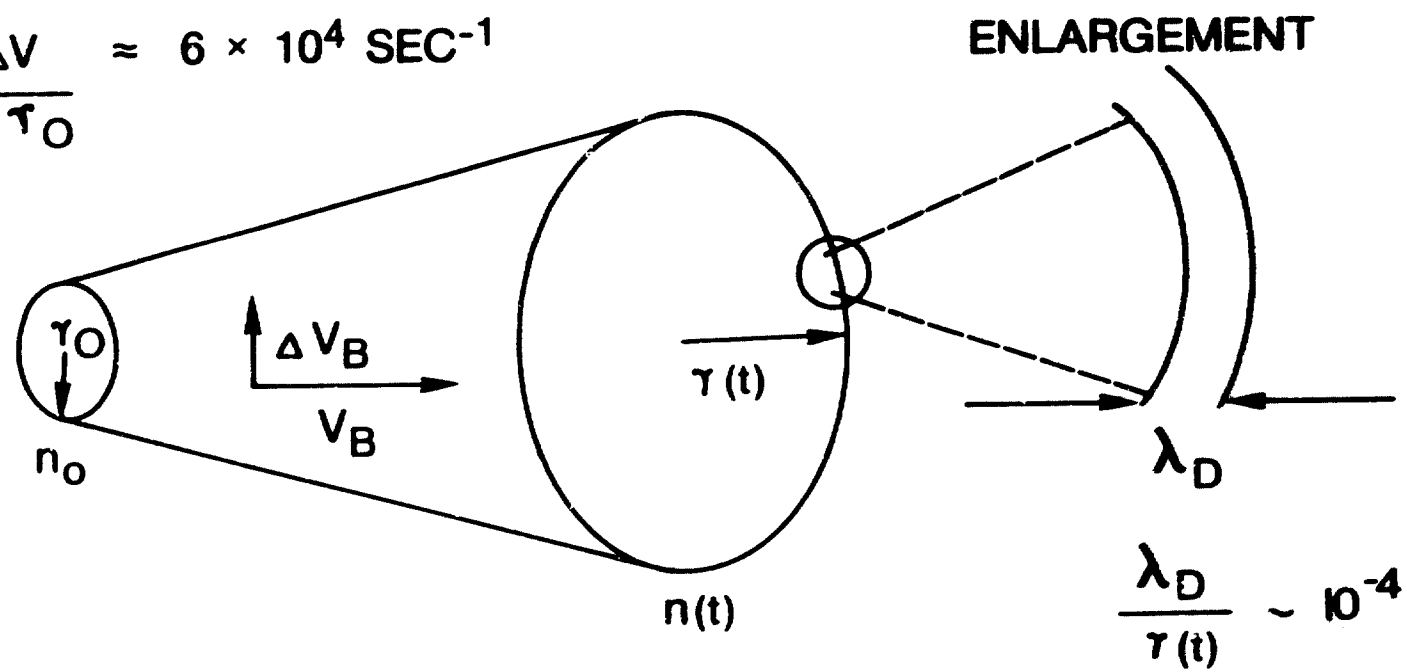

FIGURE 2

MAGNETIC FIELD DIFFUSION IN A TURBULENT ION BEAM PLASMA

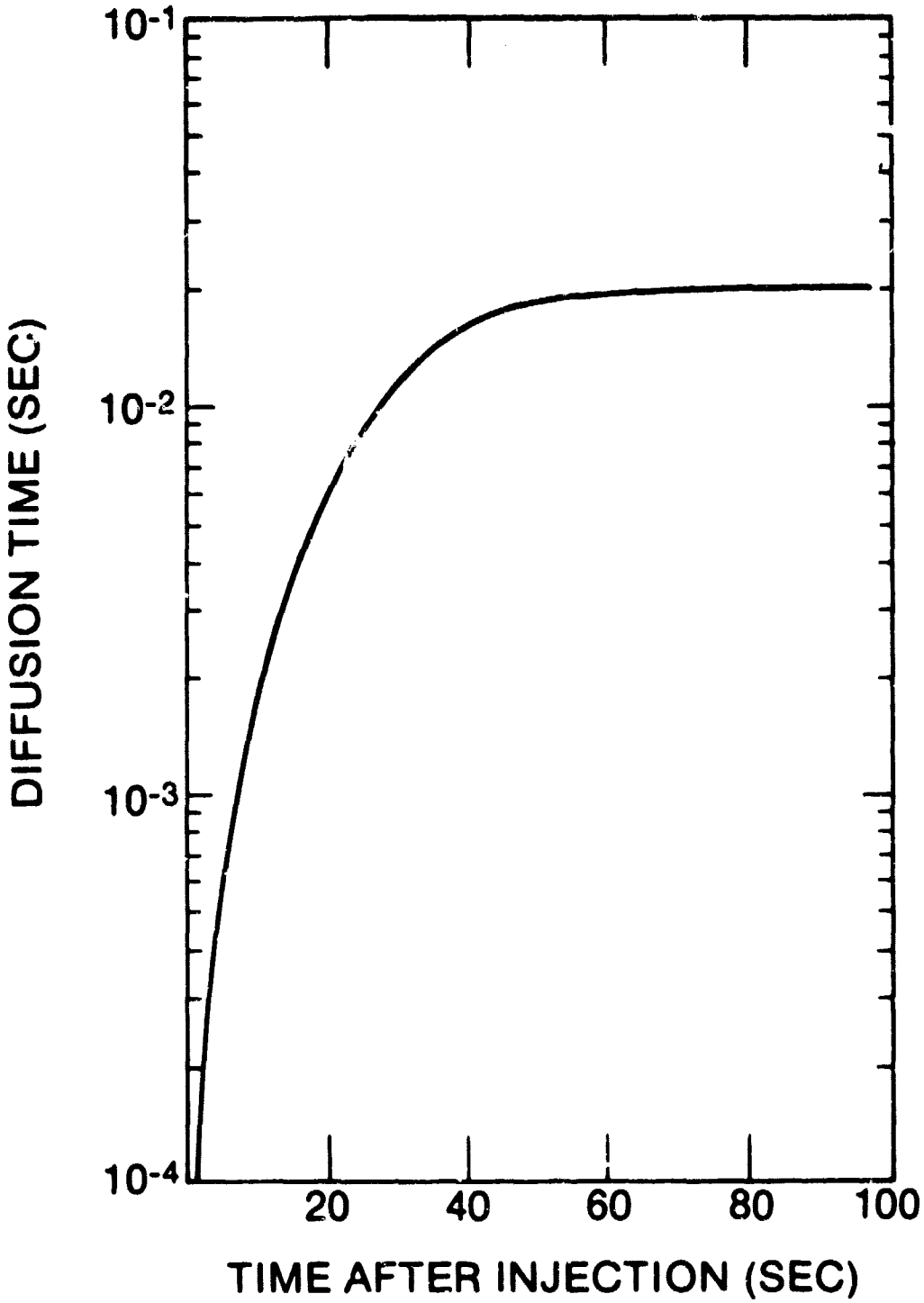

FIGURE 3

BEAM DEBYE SHEATH LOSS

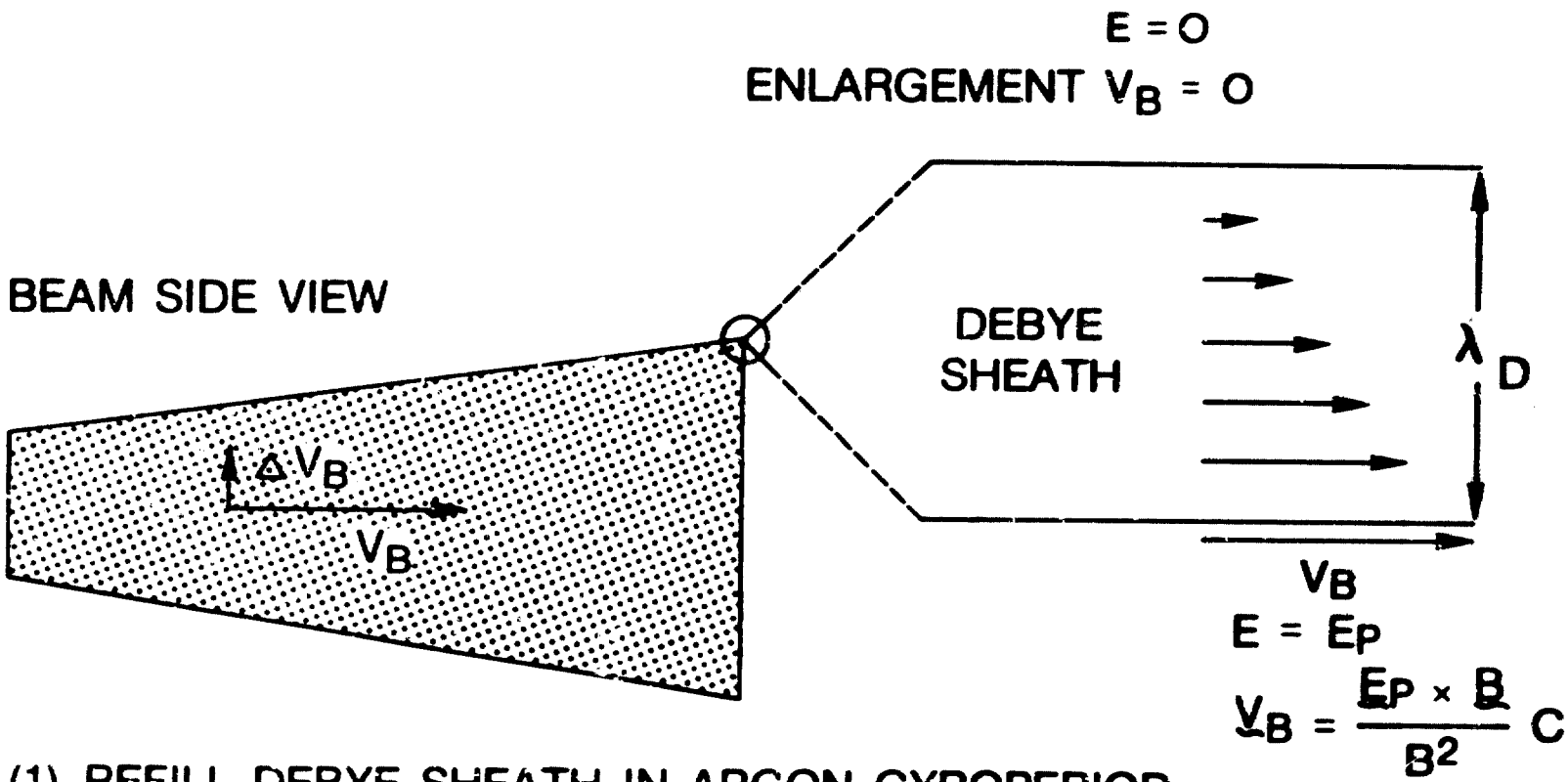

(1) REFILL DEBYE SHEATH IN ARGON GYROPERIOD

(2) SHEATH LOSS DUE TO DECREASE IN POLARIZATION FIELD, E_P, ACROSS DEBYE LENGTH

(3) SHEATH LOST EVERY GYROPERIOD

FIGURE 4

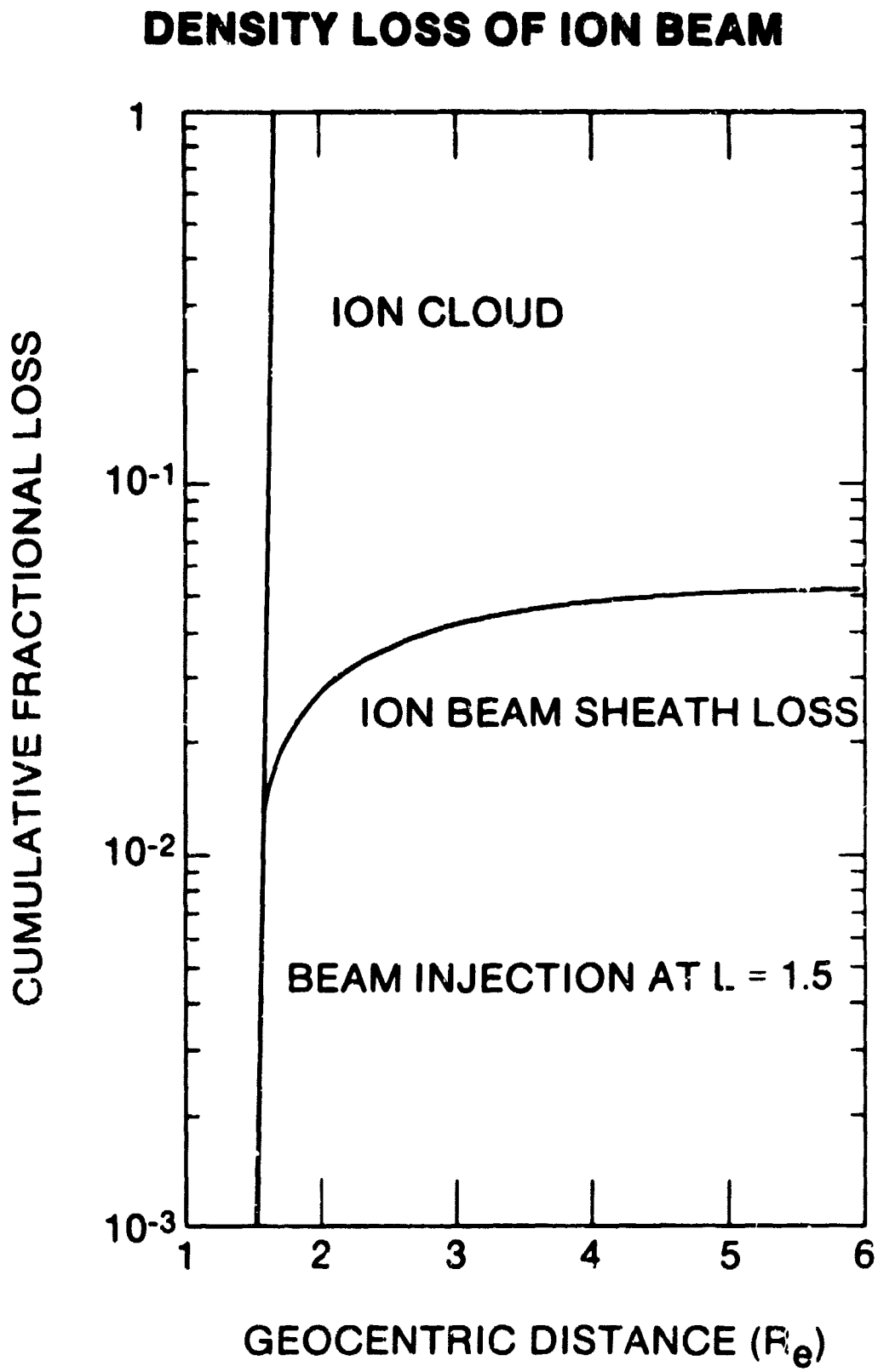
DENSITY LOSS OF ION BEAM
1
10-1
10-2
10-3
CUMULATIVE FRACTIONAL LOSS
ION CLOUD
ION BEAM SHEATH LOSS
BEAM INJECTION AT L = 1.5
1
2
3
4
5
6
GEOCENTRIC DISTANCE (Re)

FIGURE 5

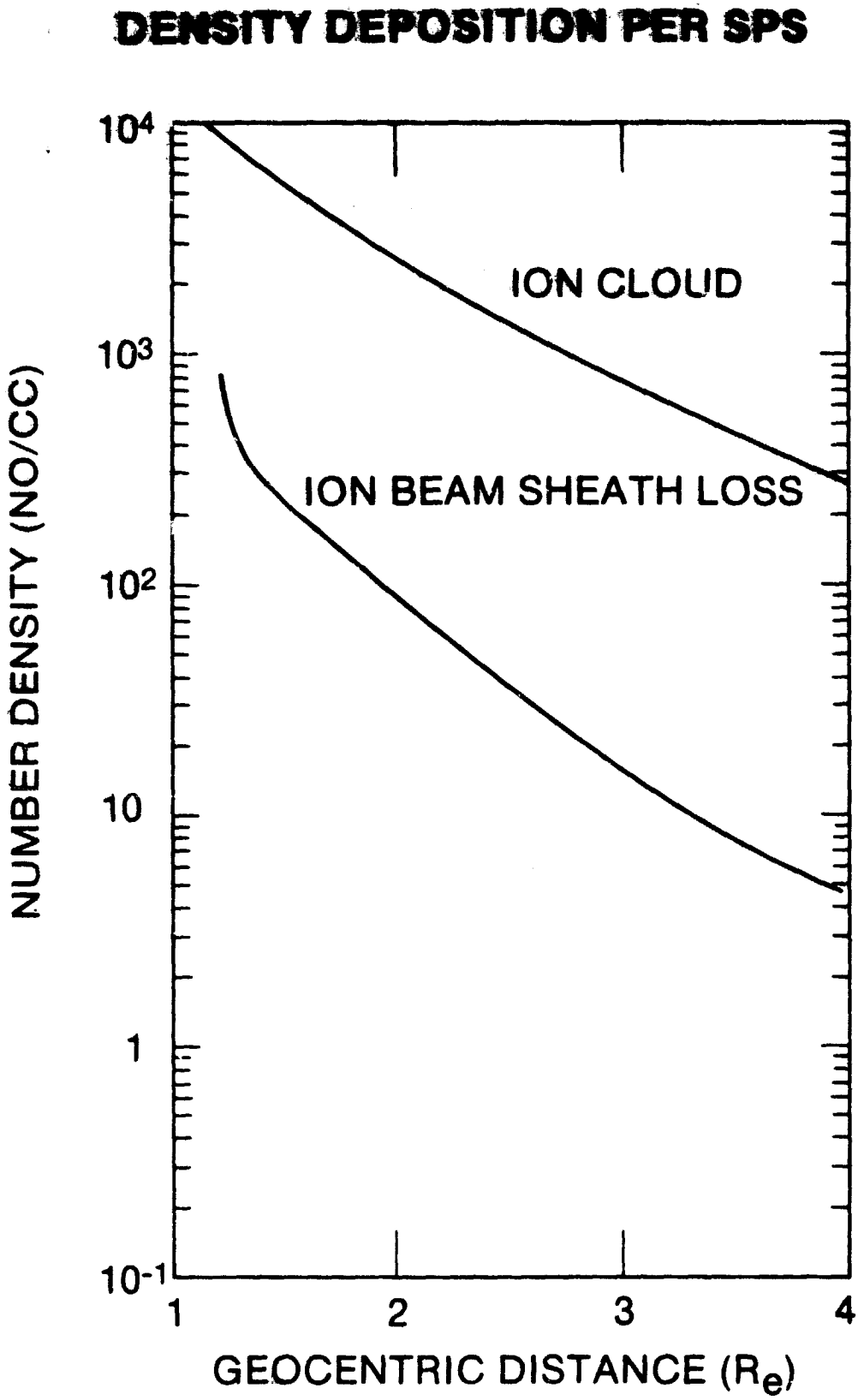
DENSITY DEPOSITION PER SPS
NUMBER DENSITY (NO/CC)
10^4
10^3
10^2
10
1
10^{-1}
ION CLOUD
ION BEAM SHEATH LOSS
1
2
3
4
GEOCENTRIC DISTANCE (R_e)

FIGURE 6

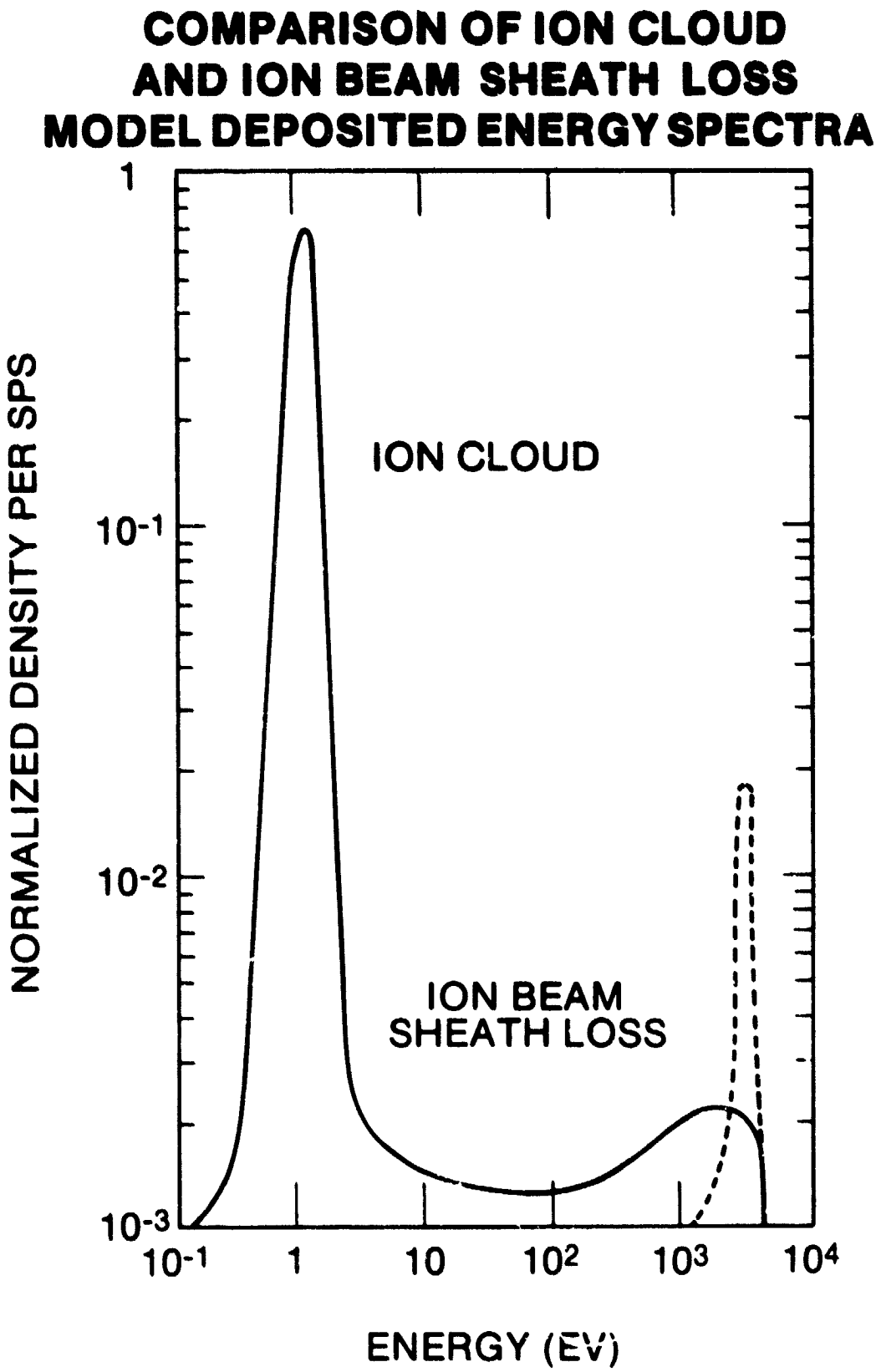
COMPARISON OF ION CLOUD
AND ION BEAM SHEATH LOSS
MODEL DEPOSITED ENERGY SPECTRA
NORMALIZED DENSITY PER SPS
1
10-1
10-2
10-3
ION CLOUD
ION BEAM
SHEATH LOSS
10-1
1
10
102
103
104
ENERGY (EV)

FIGURE 7

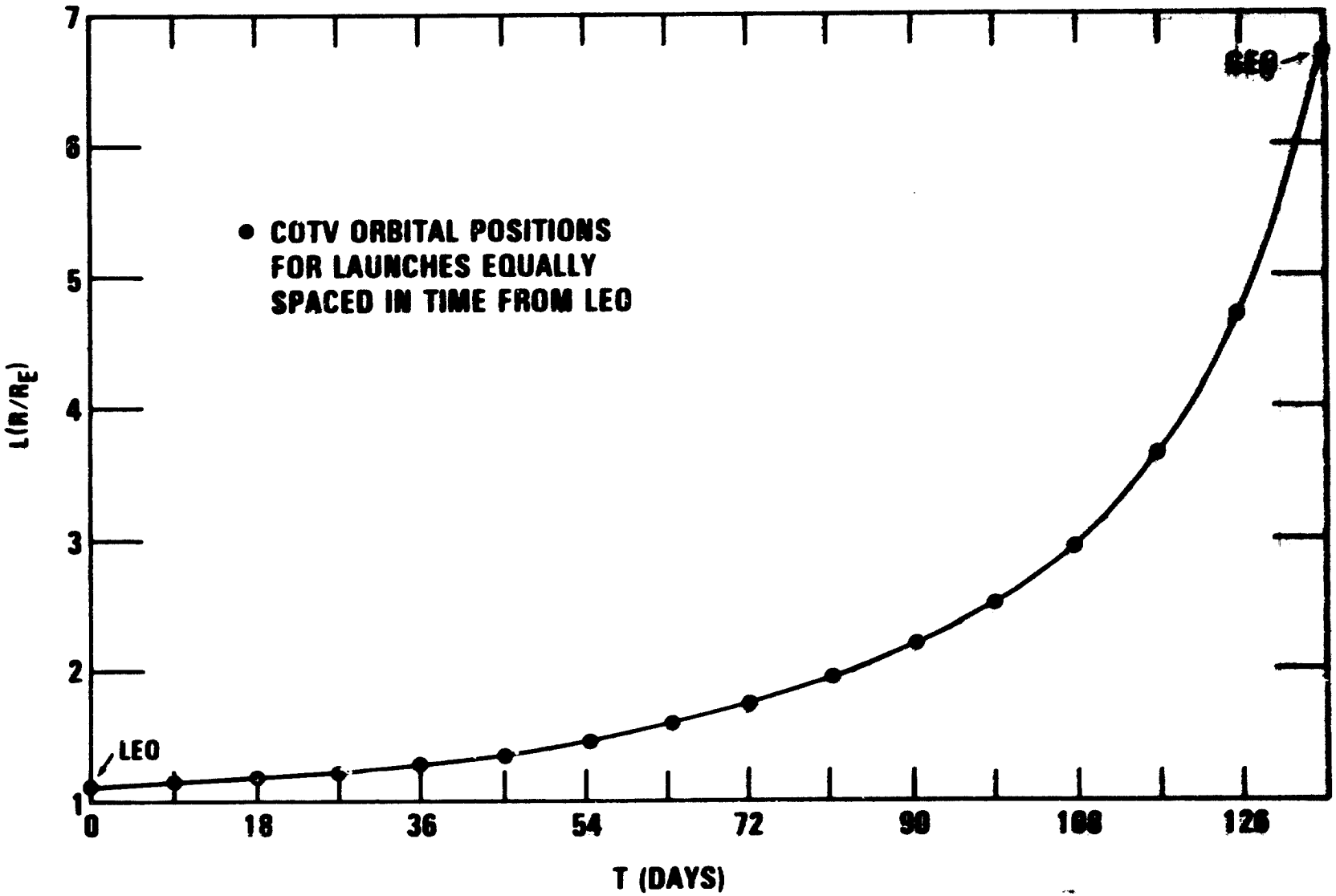

COTV ORBITAL POSITIONS
FOR LAUNCHES EQUALLY
SPACED IN TIME FROM LEO
LEO
GEO
L(R/R_E)
T (DAYS)
1
2
3
4
5
6
7
0
18
36
54
72
90
108
126

FIGURE 8

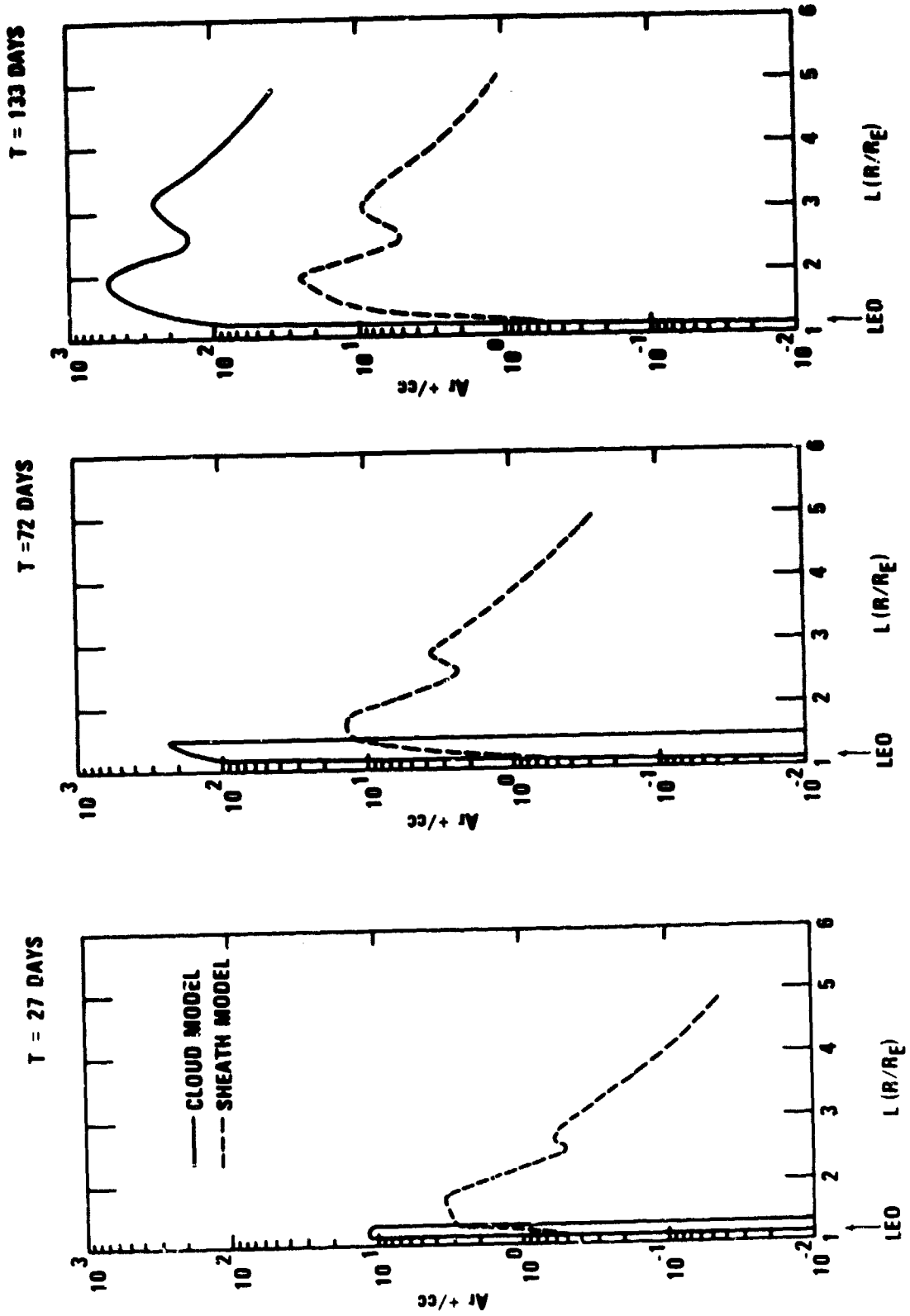
T = 27 DAYS
T =72 DAYS
T = 133 DAYS
CLOUD MODEL
SHEATH MODEL
Δf +/cc
L (R/R_E)
LEO

FIGURE 9

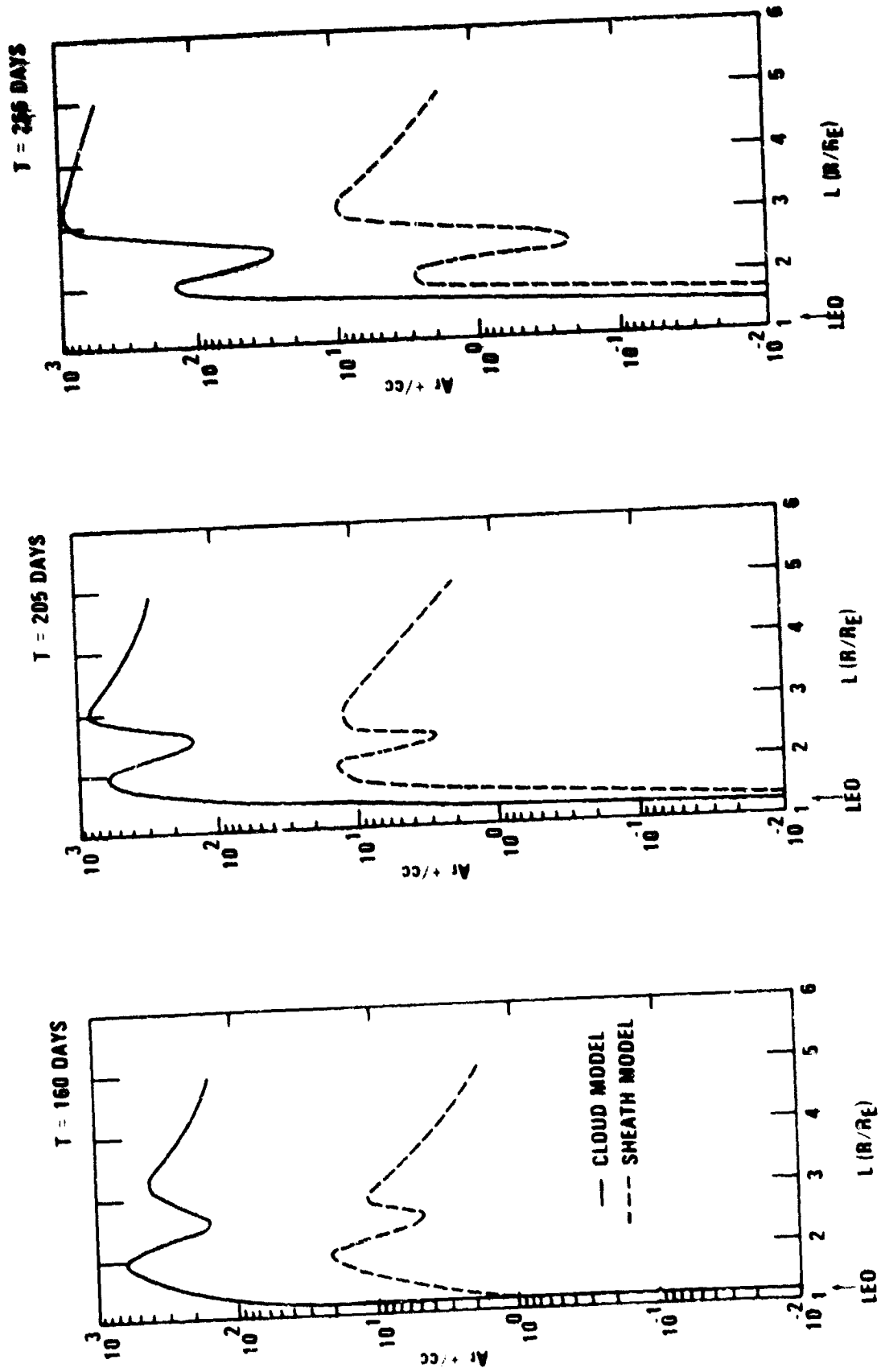
T = 160 DAYS
T = 205 DAYS
T = 295 DAYS
CLOUD MODEL
SHEATH MODEL
Δr +/cc
L (R/R_E)
LEO

FIGURE 1C